Strongly coverage-dependent excitations of adsorbed molecular hydrogen

J. A. Gupta,* C. P. Lutz, A. J. Heinrich, and D. M. Eigler
IBM Research Division, Almaden Research Center, 650 Harry Road, San Jose, California 95120, USA
(Received 1 November 2004; published 17 March 2005)

We have observed prominent nonlinearities in differential conductance spectra of H_2 on copper surfaces using a low-temperature scanning tunneling microscope. These nonlinearities result from transitions between states of H_2 with distinct conductances. Tunneling electrons drive these transitions by giving up energy to highly coverage-dependent excitations that do not correspond to known vibrational or rotational modes of H_2. The nonlinear conductance features can be modeled by extending the conventional framework for inelastic electron tunneling spectroscopy to include saturation effects.

DOI: 10.1103/PhysRevB.71.115416 PACS number(s): 68.43.−h, 68.37.−d, 67.70.+n, 67.90.+z

In his classic text on superfluids,[1] London considers why hydrogen, with an even smaller mass than helium, becomes a solid rather than a superfluid at low temperature. He explains that the greater zero-point motion of H_2 is more than offset by the greater van der Waals attraction between molecules, thus leading to a solid phase at ordinary pressure and zero temperature. Phase diagrams for hydrogen in confined geometries can be quite different than the bulk because intermolecular attractions can be weakened. For instance, it is expected that a superfluid phase of hydrogen may occur in small three-dimensional (3D) clusters[2] and in 2D clusters[3] or films[4] of hydrogen adsorbed on surfaces.

Molecular hydrogen is only weakly bound to cold, flat, noble-metal surfaces by van der Waals forces (physisorption).[5,6] We expect that the net long-range interaction between adsorbed hydrogen molecules reflects a balance between electrostatic repulsion of surface-induced dipole moments[7,8] and a van der Waals attraction weakened by dynamic screening from the surface charge density. Thus, within a range of surface coverage, it is likely that physisorbed hydrogen exhibits gas and liquid phases at temperatures well below the bulk freezing point. A variety of order-disorder transitions involving gas, liquid, and solid hydrogen phases have been observed for monolayer coverages of H_2 on graphite.[9]

Here we report excitations of adsorbed H_2 that produce highly nonlinear conductance spectra. Excitation energies increase by a factor of 3 within a range of submonolayer coverage. The sudden appearance of these excitations at a threshold coverage is suggestive of a phase transition.

Experiments were performed using ultrahigh-vacuum scanning tunneling microscopes (STM's) at temperatures of $T=5$ K and $2.5<T<18$ K. Clean surfaces of single-crystal Cu(111), Cu(100), and Cu(510) were prepared by Ar sputtering and annealing to 600 °C. No systematic differences in H_2 conductance spectra were found for these surfaces. The differential conductance dI/dV was either calculated by numerical differentiation of the tunnel current $I(V)$ or was recorded with a lock-in amplifier by adding an ac modulation (1 kHz) to the sample voltage V. H_2 gas was admitted to the room-temperature UHV chamber ($P=1\times10^{-8}$ Torr), producing a flux of H_2 incident on the sample surface. Because direct line of sight from the UHV chamber to the sample surface was blocked by a shutter held at $T=5$ K, we expect the H_2 to be cold prior to adsorption. As the low-temperature section containing the STM was not equipped to measure the surface coverage, we quote exposure times to establish a relative indication of coverage.

After ~1000 min exposure to H_2, an STM image measured at low voltage shows no visible adsorbates on the surface [Fig. 1(a)]. However, unlike the hydrogen-free Cu surface, ubiquitous noise appears in images taken at higher voltage [Fig. 1(b)]. The voltage-dependent noise is correlated with nonlinearities in the conductance. The dI/dV spectrum in Fig. 1(c) reveals a pronounced gaplike feature, with peaks that are symmetrically placed at $V_{gap}=\pm120$ mV.[10] Noise in dI/dV at $V\sim V_{gap}$ reflects two-state noise in the tunnel current. The gaplike feature and associated two-state noise are independent of the lateral tip position. As a result, STM images of the surface are uniformly noisy when taken at $V=V_{gap}$ [Fig. 1(b)].

We expect that the weak in-plane force between a physisorbed hydrogen molecule and a close-packed metal surface can be overcome by the zero-point motion of the molecule, with the consequence that the molecule will be delocalized in the plane of the surface. This is consistent with the absence of any localized adsorbates in Fig. 1. However, it is also possible that one or more H_2 molecules are confined within the STM junction, remaining so even as the tip is scanned across the surface. Thus, the ubiquitous gaplike feature may

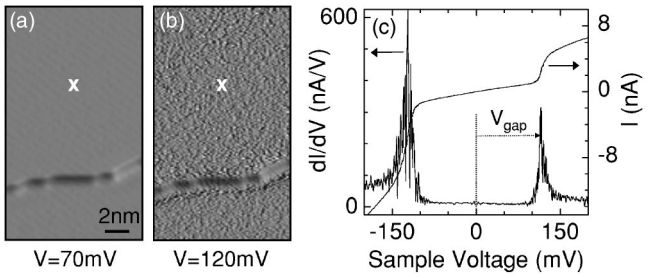

FIG. 1. Cu(111) surface with adsorbed H_2, $T=2.5$ K. (a), (b) STM images with $R=100$ MΩ. Differentiation along the horizontal axis and illumination sources are used to enhance local contrast. An atomic step is visible in the lower part of the image. × marks the tip position for the spectra in (c). (c) $I(V)$ and numerically calculated dI/dV spectra with $V=100$ mV, $I=1$ nA.

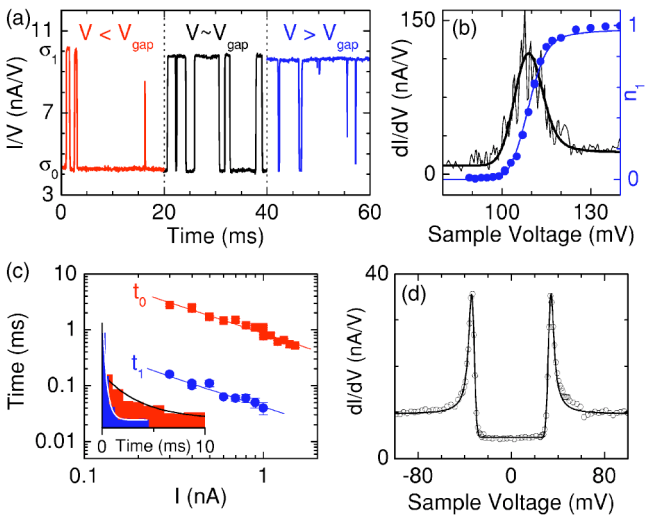

FIG. 2. (Color online) Two-state noise, $T=5$ K. H_2/Cu(111). (a) Excerpts of switching with $V=95$ mV, 109 mV, 125 mV taken at constant tip-surface separation set by $V=150$ mV, $I=1.5$ nA. (b) Left axis: numerical dI/dV showing $V_{gap}=108$ mV. Right axis: occupation fraction in the excited state. The solid lines are fits using Eqs. (4) and (5) with the parameters in Ref. 11. (c) Inset: histogram of residence times (~200 switching events) for ground and excited states from two-state noise at $V=110$ mV, $I=0.2$ nA, along with exponential fits (solid lines). Main (log-log scale): resultant mean residence times t_0 and t_1. Lines are fits with slopes of -1.0. (d) dI/dV spectrum where two-state noise cannot be resolved. Data (open symbols) taken with $V=100$ mV, $I=1$ nA, 0.5 mV_{rms} and fit (solid line) using Eq. (5) with parameters in Ref. 11. H_2/Cu(100).

result from H_2 molecules that are physisorbed on the Cu surface, are confined within the junction or a combination of both (for instance, a molecule could be switching between physisorbed and confined states).

Two-state noise in the tunnel current can be resolved by disabling the constant-current STM feedback loop. Figure 2(a) shows the repeated switching between a ground state with low conductance and an excited state with high conductance that occurs near V_{gap}. We measure the fractional occupation in ground (n_0) and excited (n_1) states at a given voltage using the relations

$$\bar{\sigma} = n_0\sigma_0 + n_1\sigma_1, \tag{1}$$

$$n_0 + n_1 = 1, \tag{2}$$

where $\sigma_0(\sigma_1)$ is the ground (excited) state conductance and $\bar{\sigma}=\bar{I}/V$ is the time-averaged conductance. The plot of excited state occupation in Fig. 2(b) indicates that the conductance peak at V_{gap} coincides with a shift in occupation from the ground to excited state. Because the conductance of each state is independent of voltage, the nonlinear dI/dV spectrum solely results from the shift in occupation between states.

To learn more about the switching mechanism, we compiled histograms of residence times in each state [Fig. 2(c), bar graph inset]. The statistical distributions are well fit by single exponentials whose decay constants are the mean residence times in ground (t_0) and excited (t_1) states. The decrease of residence times in inverse proportion to current indicates that transitions between states are driven by single tunneling electrons [Fig. 2(c)]. Together with the symmetry of dI/dV spectra about $V=0$, this trend suggests that transitions from the ground to excited state and vice versa occur by inelastic scattering.

To develop a simple zero-temperature model for the conductance of two-state systems, we extend the conventional framework of inelastic electron tunneling spectroscopy to include occupation in the excited state (i.e., saturation). Electrons elastically tunnel through the junction with conductance $\sigma_0(\sigma_1)$ when the ground (excited) state is occupied. Inelastic scattering transfers the junction from ground to excited state with an inelastic contribution to the conductance σ_{up}, provided the sample voltage exceeds a minimum value V_{mode}, corresponding to an excitation of the system (V_{gap}, for example). We consider relaxation from the excited state by inelastic scattering (with an inelastic conductance σ_{down}) and spontaneous processes (with a rate S). The tunnel current is then the sum of contributions from elastic and inelastic conductance channels:

$$\begin{aligned} I(V) &= (n_0\sigma_0 + n_1\sigma_1)V + (n_0\sigma_{up}(V - V_{mode}) + n_1\sigma_{down}V), && \text{for } V \geqslant V_{mode}, \\ I(V) &= \sigma_0 V && \text{for } V < V_{mode}. \end{aligned} \tag{3}$$

For clarity, we treat $V\geqslant 0$ with the understanding that $I(V)$ is antisymmetric about $V=0$. The fractional occupation in the excited state is

$$\begin{aligned} n_1 &= \frac{1/t_0}{1/t_0 + 1/t_1} = \frac{\sigma_{up}(V - V_{mode})}{\sigma_{up}(V - V_{mode}) + \sigma_{down}V + eS} && \text{for } V \geqslant V_{mode}, \\ n_1 &= 0 && \text{for } V < V_{mode}. \end{aligned} \tag{4}$$

After substituting Eqs. (2) and (4) into Eq. (3), we obtain the differential conductance

$$\begin{aligned} \frac{dI}{dV} &= A + \frac{B}{[1 + (V - V_{mode})/V^*]^2} && \text{for } V \geqslant V_{mode}, \\ dI/dV &= \sigma_0 && \text{for } V < V_{mode}, \end{aligned} \tag{5}$$

where A, B, and V^* are voltage-independent functions of the parameters σ_0, σ_1, σ_{up}, σ_{down}, V_{mode}, and S :

$$A = [\sigma_{up}(\sigma_1 + \sigma_{down}) + \sigma_{down}(\sigma_0 + \sigma_{up})]/(\sigma_{up} + \sigma_{down}), \tag{6}$$

$$B = \frac{\sigma_{up}[(\sigma_{up}V_{\text{mode}} - eS)(\sigma_1 - \sigma_0) + 2\sigma_{up}\sigma_{down}V_{\text{mode}} + eS(\sigma_{up} - \sigma_{down})]}{(\sigma_{down}V_{\text{mode}} + eS)(\sigma_{up} + \sigma_{down})}, \tag{7}$$

$$V^* = (\sigma_{down}V_{\text{mode}} + eS)/(\sigma_{up} + \sigma_{down}). \tag{8}$$

Equation (5) yields a gaplike feature when $\sigma_1 > \sigma_0$ and predicts an asymmetric line shape characterized by a sudden rise in dI/dV at $V = V_{\text{mode}}$ followed by a more gradual decay set by V^*. This asymmetric line shape can occur even when σ_{up} and σ_{down} are very small, as long as the spontaneous relaxation rate S is comparably small. Analysis of this line shape gives information on the spontaneous relaxation rate and inelastic channel strengths. Because the onset at $V = V_{\text{mode}}$ in the model is infinitely sharp, it is necessary to introduce broadening before using Eq. (5) to fit the dI/dV spectra. We find that convolution of Eq. (5) with a Gaussian distribution about V_{mode} sufficiently approximates contributions from thermal and inhomogeneous broadening to fit our data.

Figure 2(b) includes calculated curves using Eqs. (4) and (5) with parameters in Ref. 11. The agreement between the data and fit is good but broadening for these data dominates the asymmetry proposed by Eq. (5). As a result, the fit parameters are not well determined. Broadening of the conductance peaks in Fig. 2(d) is sufficiently small that a distinctly asymmetric line shape is observed in agreement with Eq. (5).[11] Switching rates for this particular junction greatly exceed the STM bandwidth (~100 kHZ), so that two-state-related noise is absent in the conductance peaks. The fit constrains the spontaneous relaxation rate, $0.5 < S < 2.5$ GHz, indicating that relaxation from the excited state is not entirely driven by tunneling electrons in this case.

Comparison of Figs. 2(b) and 2(d) indicates that V_{gap} and switching rates vary considerably. Discussed further below, the two most relevant changes in experimental conditions between these spectra are differences in the atomic structure of the tip and in the hydrogen surface coverage. We note the deceptive resemblance of Fig. 2(d) to the quasiparticle excitation spectrum of a BCS superconductor. Equation (5) shows how a saturable two-state system can exhibit a differential conductance spectrum with this general shape.

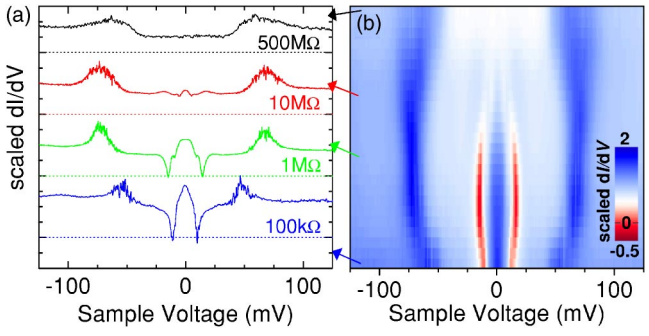

FIG. 3. (Color online) Emergence of NDR. Decreasing the junction resistance $R = V/I$ by one decade moves the tip closer to the surface by ~0.1 nm. All data are scaled by R. The tip height was set at $V = 100$ mV. (a) Dotted lines indicate zero conductance for each scan. From top to bottom, $V_{\text{rms}} = 2$, 1, 0.5, 0.2 mV. (b) Complete series with 500 MΩ > R > 100 kΩ. H_2/Cu(111), $T = 5$ K.

Figure 3 shows that an additional conductance feature emerges at low voltage as the tip is brought closer to the surface. For junction resistances $R < 20$ MΩ, symmetric dips appear that exhibit (typically pronounced) negative differential resistance (NDR). The NDR feature originates from repeated transitions between two states in a fashion similar to the gaplike feature (Fig. 4). Dips (rather than peaks) in dI/dV occur at $V = \pm V_{\text{ndr}}$ because the relevant excited-state conductance is *lower* than the ground-state conductance ($\sigma_1 < \sigma_0$).[12] The NDR feature appears regardless of lateral tip position and exhibits a variability in switching rates that is comparable to the gaplike feature [e.g., Figs. 4(a) and 4(b)]. The coexistence of gaplike and NDR features in Fig. 3 indicates that at least three states of H_2 are present. Equation (5) can be extended to such a situation by including two modes at V_{gap} and V_{ndr} or by considering gaplike and NDR features as independent two-state systems.

In considering physical origins for the states and excita-

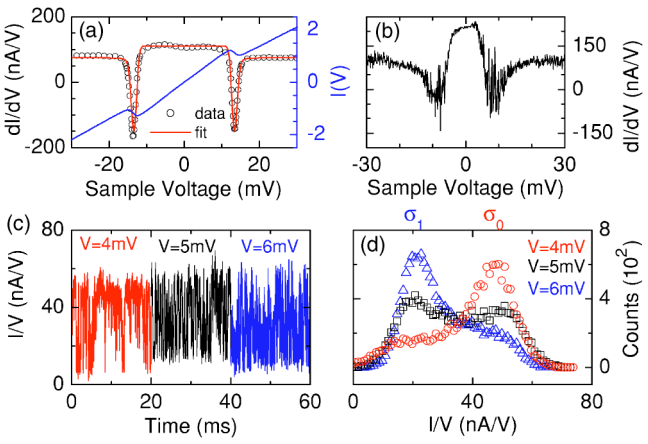

FIG. 4. (Color online) (a) dI/dV (open symbols) and associated $I(V)$ (dotted line) where two-state switching occurs too quickly to be resolved. The solid line is a fit using Eq. (5) with $\sigma_0 = 110.8$ nA/V, $A = 74.1$ nA/V, $B = -17.0$ μA/V, $V^* = 0.03$ mV, $V_{\text{mode}} = 13.3$ mV, broadening = 0.8 mV. (b) NDR with switching noise that can be resolved, taken with a different tip and surface coverage than the data in (a). (c) Excerpts of two-state noise near V_{ndr}. (d) Corresponding histogram showing $\sigma_1 < \sigma_0$. H_2/Cu(111), $T = 5$ K, $V = 10$ mV, $I = 1$ nA, 0.5 mV_{rms}.

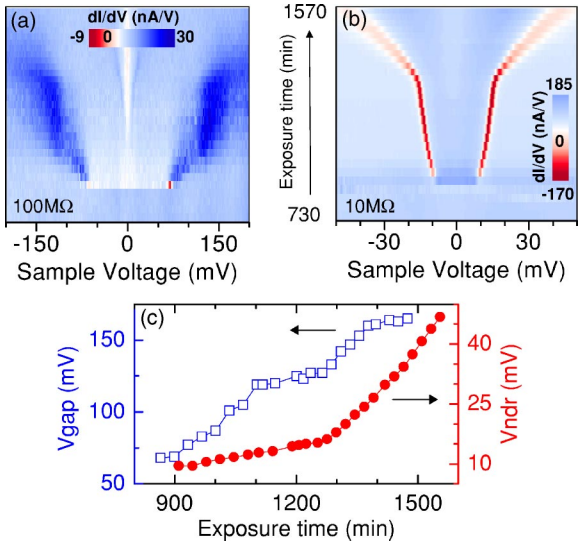

FIG. 5. (Color online) Sudden onset and shifts of gaplike and NDR features with exposure. (a) dI/dV with $R=100$ MΩ ($V=100$ mV, $I=1$ nA, 0.5 mV_{rms}). (b) $R=10$ MΩ ($V=10$ mV, $I=1$ nA, 0.5 mV_{rms}). (c) V_{gap} and V_{ndr} from (a), (b)H_2/Cu(111), $T=5$ K.

tions responsible for gaplike and NDR features, we note that two different interpretations of excitation energies are consistent with our spectra. In the model presented above, V_{mode} is equal to the energy difference between ground and excited states. However, the functional form of Eq. (5) is unchanged if one instead considers a "double-well" system where V_{mode} corresponds to the energy difference between the ground state and an intermediary transition state.

In a prior STM study of NDR,[12] the high- and low-conductance states corresponded to different molecular conformations. Switching between these states was driven by inelastic excitations of a vibrational mode. Thus, a higher-lying vibrational level served as a transition state and V_{ndr} was equal to a vibrational energy. It is unlikely that V_{gap} or V_{ndr} in our measurements corresponds to known excitations of physisorbed or chemisorbed H_2 in part because we observe large shifts with exposure that have not been reported previously.[6,7,13–15] To monitor these shifts, the tip was positioned over a clean terrace and dI/dV spectra were recorded as a function of exposure time t. Spectra taken with $t<860$ min were unchanged from the clean Cu surface. Figures 5(a) and 5(b) indicate that gaplike and NDR features suddenly appear with $V_{gap}=80$ mV and $V_{ndr}=11$ mV at $t\sim900$ min.[16] This onset time is reproducible to ~20%, suggesting that a threshold coverage of H_2 is necessary before gaplike and NDR features are observed. Subsequent spectra reveal that V_{gap} and V_{ndr} continuously increase with exposure [Fig. 5(c)]. Our ability to monitor this trend is limited by concurrent broadening of both features. Within our entire data set, V_{gap} and V_{ndr} span an order of magnitude: $25<V_{gap}<280$ mV and $8<V_{ndr}<80$ mV. Similar values were observed for HD and D_2 ; it is difficult to establish whether small isotope shifts occur. The STM images in Fig. 6 show the formation of ordered regions for $t>2000$ min, suggestive of monolayer coverage. Because neither gaplike nor NDR features are distinguishable at this exposure, it is likely that gaplike and NDR features occur at submonolayer H_2 coverage.

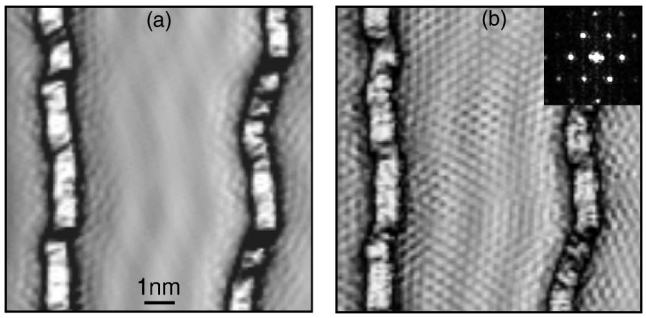

FIG. 6. Incommensurate ordering of H_2 on Cu(111) for long exposure times $t>2000$ min. (a) STM image with ($V=10$ mV, $I=1$ nA). Ordered regions grow outward from step edges. (b) Image of the same area with additional exposure to H_2. A hexagonal pattern is visible with a nearest-neighbor spacing of 0.38 ± 0.01 nm consistent with bulk solid hydrogen. Inset: fast Fourier transform of the terrace region. $T=5$ K.

The dependence on tip-surface separation in Fig. 3 indicates that the presence of the STM tip plays a role in gaplike and NDR features. We find that dI/dV spectra change markedly when the atomic structure of the tip apex is perturbed (Fig. 7). Thus, the variability in excitation energies[16] and switching rates can be attributed to changes in the apex due to tip preparation. We have observed gaplike and NDR features up to $T=18$ K. H_2 completely desorbs from the surface at $T\sim25$ K, providing a way to repeat exposures without additional surface and tip preparation. In this way, we verified that excitation energies and conductance states are repro-

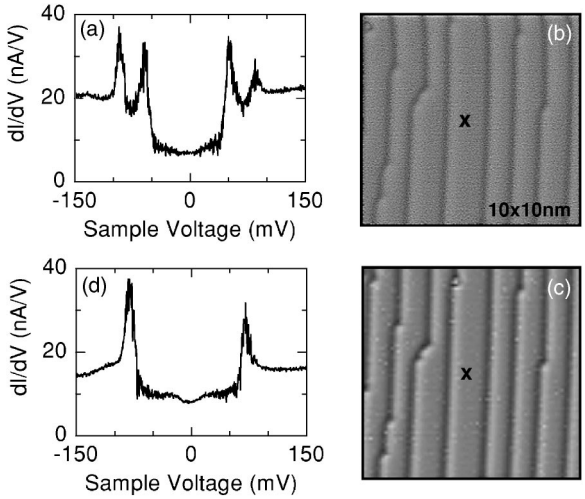

FIG. 7. Changes in spectra due to perturbation of the tip apex. (a) Initial spectrum upon exposure to H_2 showing two well-resolved gaplike features. (b) Corresponding image taken at $V=90$ mV, $I=0.9$ nA. Graininess in the image reflects switching noise as in Fig. 1(b). (c) STM image of the same area after the tip apex is perturbed by physical contact with the surface. (d) Associated dI/dV spectrum. dI/dV spectra in (a), (d) were taken with the tip positioned at × in (b), (c) with $V=20$ mV, $I=0.2$ nA, 1 mV_{rms}, H_2/Cu(510), $T=5$ K.

duced when the exact atomic structure of the tip is kept intact. We note that Cu is the only metal where both gaplike and NDR features appear concurrently. We have observed NDR features from hydrogen on Ni(110), NiAl (110), Pt (111), and Ag(111).

Our observations suggest that the excitations and conductance states are associated with hydrogen in the STM junction and cannot be attributed to hydrogen adsorbed solely on either surface or tip. This explains the dissonance between our measurements and prior electron beam inelastic scattering experiments.[6,7,13,14] If a small number of molecules are confined to the junction, conductance states could reflect different relative conformations among molecules, varying numbers of confined molecules, or distinct adsorption states within the junction. Excitations by tunneling electrons could then drive a change in conformation, add or subtract a molecule from the junction, or induce a change in adsorption site. Hindrance of molecular motion by surrounding H_2 molecules adsorbed on the tip and surface could continuously increase the energy barrier required for changes in adsorption or conformation states, accommodating the trends in Fig. 5. Alternative scenarios involving dissociative electron attachment[17] or where hydrogen molecules within the STM junction condense to form 3D clusters or 2D films are also plausible. Condensed hydrogen in the junction may exhibit a variety of density-dependent phase transitions (gas/liquid/solid, order/disorder,[9] or even superfluid.[2–4]) The threshold coverage suggested by Fig. 5 is consistent with a phase transition. To our knowledge, quantitative predictions of collective excitations in such nanoscale condensates are not available at present.

We thank C.T. Rettner, A.F. Panchula, and M.W. Hart for their help and acknowledge support from the Defense Advanced Projects Research Agency.

*Corresponding author.
Electronic address: jgupta@mps.ohio-state.edu

[1] F. London, *Superfluids* (Dover, New York, 1964), Vol. 2, pp. 33–35.
[2] P. Sindzingre, D. M. Ceperley, and M. L. Klein, Phys. Rev. Lett. **67**, 1871 (1991); S. Grebenev, B. Sartakov, J. P. Toennies, and A. F. Vilesov, Science **289**, 1532 (2000).
[3] M. C. Gordillo and D. M. Ceperley, Phys. Rev. B **65**, 174527 (2002).
[4] M. C. Gordillo and D. M. Ceperley, Phys. Rev. Lett. **79**, 3010 (1997).
[5] Ph. Avouris, D. Schmeisser, and J. E. Demuth, Phys. Rev. Lett. **48**, 199 (1982).
[6] S. Andersson and J. Harris, Phys. Rev. Lett. **48**, 545 (1982).
[7] K. Svensson and S. Andersson, Phys. Rev. Lett. **78**, 2016 (1997).
[8] J. K. Nørskov, A. Houmøller, P. K. Johansson, and B. I. Lundqvist, Phys. Rev. Lett. **46**, 257 (1981).
[9] H. Wiechert, Physica B **169**, 144 (1991).
[10] The positions of conductance peaks are not always completely symmetric about $V=0$; systematic deviations may reflect a dependence of excitations on electric field within the junction.
[11] Fit parameters in Fig. 2(b) are $\sigma_0=8.6$ nA/V, $A=20.9$ nA/V, $B=1724$ nA/V, $V^*=0.8$ mV, $V_{\mathrm{mode}}=108$ mV, and broadening =4.4 mV. Fit parameters in Fig. 2(d) are $\sigma_0=4.5$ nA/V, $A=9.7$ nA/V, $B=100$ nA/V, $V^*=2.3$ mV, $V_{\mathrm{mode}}=32.2$ mV, and broadening =1.8 mV.
[12] J. Gaudioso, L. J. Lauhon, and W. Ho, Phys. Rev. Lett. **85**, 1918 (2000).
[13] L. Bengtsson, K. Svensson, M. Hassel, J. Bellman, M. Persson, and S. Andersson, Phys. Rev. B **61**, 16921 (2000).
[14] K. Svensson, L. Bengtsson, J. Bellman, M. Hassel, M. Persson, and S. Andersson, Phys. Rev. Lett. **83**, 124 (1999).
[15] R. H. M. Smit, Y. Noat, C. Untiedt, N. D. Lang, M. C. Van Hemert, and J. M. van Ruitenbeek, Nature (London) **419**, 906 (2002).
[16] In ~20 independent experiments where the onset of gaplike and NDR features was resolved, V_{gap} began in the range 25–90 mV while V_{ndr} more reliably began at 11 ± 2 mV.
[17] M. Allan and S. F. Wong, Phys. Rev. Lett. **41**, 1791 (1978).